# GTOC9: Results from the National University of Defense Technology

Yazhong Luo*, Yuehe Zhu, Hai Zhu, Zhen Yang,

Shuai Mou, Jin Zhang, Zhenjiang Sun, and Jun Liang

*College of Aerospace Science and Engineering, National University of Defense Technology, Changsha 410073, China*

**Abstract:** The ninth edition of the Global Trajectory Optimization Competition (GTOC) series was successfully organized in April 2017, wherein the competitors were called to design a series of missions able to remove a set of 123 orbiting debris pieces while minimizing the overall cumulative cost. A three-level optimization framework is presented to solve the complex problem, which combines the dynamic Travelling Salesman Problem (TSP), mixed-integer sequence optimization and perturbed trajectory rendezvous optimization. The framework was employed by the NUDT team during GTOC9, and the corresponding result ranked second in the eventual leaderboard.

## I. Introduction

The design of space trajectories can be profitably approached as a global optimization problem. The optimal trajectory, which is significant for practical space mission design, is usually very difficult to be obtained. The Global Trajectory Optimization Competition (GTOC) series [1], was born with the objective of fostering research in this area by letting the best aerospace engineers and mathematicians worldwide challenge themselves to solve one, difficult, well-defined, problem of interplanetary trajectory design.

The GTOC9 [2] was successfully organized in April 2017 by the Advanced Concepts Team (ACT) of European Space Agency (ESA), who won the GTOC8. For calling to protect the environment of earth orbits, the background of the GTOC problem is put in the near-earth space for the first time. The competitors are called to design a series of missions able to remove a set of 123 orbiting debris pieces while minimizing the overall cumulative cost.

To find the optimal solution of such a complex problem, three sub-problems need to be extracted and solved. 1) First, the set of 123 debris pieces needs to be divided into several groups. Each group of debris is removed by one mission. Optimization is performed to minimize the overall cumulative cost. This can be approached as a dynamic TSP and solved by some evolution algorithm [3]. 2) Second, given a group of the debris, one mission is designed by mixed-integer optimization to remove them while costing minimal velocity increment [4]. 3) Finally, given the current and next debris as well as the rendezvous duration, the impulsive maneuver strategy is designed to produce the optimal flight trajectory [5].

This paper presents a three-level optimization framework to solve the above problem. The framework was employed by the team of National University of Defense Technology(NUDT) in GTOC9. The result ranked second in the eventual leaderboard, only behind the amazing result from Jet Propulsion Laboratory (JPL).

## II. Problem Statement

### A. Problem Description

Since the launch of the first satellite, Sputnik, in 1957, mankind has placed countless spacecraft in orbit around the Earth. Today, less than 10% of the trackable objects orbiting the Earth are operational satellites. The remainder is simply junk, and this space debris is becoming an increasingly serious problem. Following the unprecedented explosion of a Sun-synchronous satellite, the Kessler effect triggered further impacts and the Sun-synchronous orbits environment was severely compromised [2]. Scientists from all main space agencies and private space companies isolated a set of 123 orbiting debris pieces that, if removed, would restore the possibility to operate in that precious orbital environment and prevent the Kessler effect to permanently compromise it.

Therefore, the problem of GTOC9 is to design $n$ missions able to cumulatively remove all the 123 orbiting debris while minimizing the overall cumulative cost of such an endeavor. One mission is a multiple-rendezvous spacecraft trajectory where a subset of size $N$ of the 123 orbiting debris is removed by the delivery and activation of $N$ de-orbit packages. The following cost function has to be minimized:

$$J = \sum_{i=1}^{n} C_i = \sum_{i=1}^{n} \left[ c_i + \alpha \left( m_{0_i} - m_{dry} \right)^2 \right]$$
$$c_i = c_m + \frac{t_{submission} - t_{start}}{t_{end} - t_{start}} (c_M - c_m) \tag{1}$$

* Corresponding author: E-mail: luoyz@nudt.edu.cn.

where $C_i$ is the cost charged by the contracted launcher supplier for the $i^{th}$ mission. At the beginning of the $i^{th}$ mission, $m_{0_i}$ is the spacecraft mass and $m_{dry}$ its dry mass. Each spacecraft initial mass $m_0$ is the sum of its dry mass, the weights of the $N \geq 1$ de-orbit packages to be used and the propellant mass: $m_0 = m_{dry} + Nm_{de} + m_p$ . All spacecraft have a dry mass of $m_{dry} = 2000$ [kg] and a maximum initial propellant mass of $m_p = 5000$ [kg] (less propellant may be used, in which case the launch costs will decrease). Each de-orbit package has a weight of $m_{de} = 30$ [kg]. The $\alpha$ parameter is set to be $\alpha = 2.0 \cdot 10^{-6}$ $[MEUR / Kg^2]$ . $t_{submission}$ is the epoch at which the $i^{th}$ mission is validated, and $t_{end}$ and $t_{start}$ are the end and the beginning epochs of the GTOC9 competition. The minimal basic cost $c_m$ is 45 MEUR, while the maximum cost $c_M$ is 55 MEUR. The other detailed constraints defined by the organizer are given in [2].

During each transfer between two successive debris, the spacecraft dynamics is described, by a Keplerian motion perturbed by main effects of an oblate Earth, i.e. $J_2$ .

$$\begin{cases} \dot{x} = v_x, \quad \dot{y} = v_y, \quad \dot{z} = v_z \\ \dot{v}_x = -\dfrac{\mu x}{r^3} + \dfrac{3\mu J_2 R_E^2}{2r^5}\left(\dfrac{5z^2}{r^2} - 1\right)x + \Gamma_x \\ \dot{v}_y = -\dfrac{\mu y}{r^3} + \dfrac{3\mu J_2 R_E^2}{2r^5}\left(\dfrac{5z^2}{r^2} - 1\right)y + \Gamma_y \\ \dot{v}_z = -\dfrac{\mu z}{r^3} + \dfrac{3\mu J_2 R_E^2}{2r^5}\left(\dfrac{5z^2}{r^2} - 3\right)z + \Gamma_z \end{cases} \quad (2)$$

where $\boldsymbol{r} = [x, y, z]^T$ and $\boldsymbol{v} = [v_x, v_y, v_z]^T$ are the spacecraft's position and velocity vector described in the mean equator inertial coordinate system of the center body, $r = \| \boldsymbol{r} \|$, $\|\cdot\|$ denotes the Euclidean norm of a vector, $\mu$ , $R_E$ and $J_2$ are the gravitational constant, mean equator radius and $J_2$-perturbation coefficient of the central body respectively. $\boldsymbol{\Gamma}$ is the thrust acceleration.

The only maneuvers allowed to control the spacecraft trajectory are instantaneous changes of the spacecraft velocity (its magnitude being denoted by $\Delta V$ . After each such maneuver, the spacecraft mass is to be updated using Tsiolkovsky equation:

$$m_f = m_i \exp\left(-\frac{\Delta V}{v_e}\right), \quad (3)$$

where $v_e = I_{sp} g_0$ . A maximum of 5 impulsive velocity changes is allowed during each transfer between two successive debris. These do not include the departure and arrival impulse.

According to Eq. (1), the following three steps are required to compute the cost function of GTOC9 problem.

**Step 1)**: Determine the number of missions (i.e. $n$) and the number of debris in each mission (i.e. $N_i$), so that $\sum_{i=1}^{n} N_i = 123$ .

**Step 2)**: Determine the rendezvous sequence from debris to debris in one mission.

**Step 3)**: Determine the transfer trajectory from debris to debris in one mission, i.e., to compute the maneuver time and impulses so that the spacecraft can sucessfully transfer from the first debris to the last one under the given constraints.

As an intermediate procedure, Step 2) and be handled together with Step 1) or with Step 3). In order to efficiently obtain a near-optimal solution, we solve the GTOC9 problem using all of these three steps, they are introduced in Secs. IV, V, and VI, respectively.

## B. Problem Analysis

The GTOC9 problem is to design a series of missions with minimal propellant costs, for the objective of removing the given 123 orbiting debris. In order to find the optimal debris-removal plan, the following three sub-problems must be addressed:

1）How to plan the successive removal missions?

2）How to minimize the cost of a single mission?

3）How to optimize the trajectory between each two debris?

The first sub-problem is a large-scale multi-sequence combinatorial optimization problem, which is similar to the combination of the classic travelling salesman problem (TSP) and bin packing problem (BPP). The TSP is to find a closed minima-distance path, with the constraints that all nodes should be visited once and only once. The BPP is to find the minimum number of packages, so that all the items can be packed. However, compared with TSP and BPP, the following differences make this sub-problem more difficult.

In the BPP, only weight constraints need to be satisfied, and the sequence of each item does not affect the weight of a package. However, for the GTOC9 problem, both the items (debris) themselves and their package sequence will significantly affect the cost function, which makes the solution space much larger than BPP, and thus leads to difficulties on optimization.

Additionally, in comparison to the TSP, the GTOC9 problem can be divided into an unlimited number of missions, and the route of debris removal can be discontinuous between every two missions. Once again it makes the solution space of this problem much larger than the TSP, and increases the difficulties of optimizing as well.

In the TSP, all the nodes to be visited are fixed in the plane and the cost of going from one node to another can be easily calculated according to the Cartesian distance in the plane. While for the GTOC9 problem, the cost of going from one debris to another depends on the respective starting date and arrival date. This further makes the problem time-dependent and difficult.

The second sub-problem is a mixed-integer nonlinear-programming (MINLP) problem, in which both the sequence (integer variables) of the debris and the transfer times (real variables) between every two debris need to be regarded as design variables. Therefore, it becomes more difficult to solve than either mixed-integer linear-programming (MILP) cases and nonlinear-programming (NLP) cases.

The third sub-problem is an orbital transfer problem. With the authors' best knowledge, it is almost impossible to accurately compute the $\Delta V$ and the detailed maneuver plan $(t_i, \Delta \mathbf{v}_i), i = 1, 2, ..., K$ in sub-problems 1) and 2) in a personal computer, due to the huge computation time. The best choice is to approximately estimate the $\Delta V$ cost in sub-problems 1) and 2) to efficiently determine the number of missions and the rendezvous sequence in each mission, then to optimize the accurate maneuver plan $(t_i, \Delta \mathbf{v}_i), i = 1, 2, ..., K$ .

There are two challenges in solving the third sub-problem. First, it is difficult to estimate the $\Delta V$ cost and the flight time $t_f$ with a relatively high precision for a single rendezvous mission between two debris. This is because that a big the right ascension of ascending node (RAAN) difference may exist between two debris, and the economic way to correct this big out-of-plane difference is to make use the natural orbital precession rate due to the central body's $J_2$-perturbation [7]. As a result, the in-plane maneuvers couples with the out-of-plane maneuvers, and a compromising exists between the rendezvous time $t_f$ and the $\Delta V$ cost. If no optimization is permitted for the consideration of computation time, an accurate estimation of $t_f$ and $\Delta V$ is a challenging work. We will introduce our estimation method in Sec. IV.C.

Secondly, it is difficult to find the optimal solution for the long-duration ( $t_f$ is up to 30 days) $J_2$-perturbed rendezvous problem. When the $J_2$-perturbation is taken into account, the well-known orbital targeting algorithms such as the Lambert algorithm will be failed in obtaining the feasible solutions, and the constrained optimization methods which can directly corporate final state constraints, such as the sequential quadratic programming (SQP), will also encounter convergence problems for long-duration rendezvous. From the scope of orbital dynamics, at least two impulses are needed to target the final position and velocity vectors. However, the total velocity increment of the 2-impulse maneuvers will be very large for a rendezvous mission, especially for long-duration, large non-coplanar rendezvous problems. Therefore, a rendezvous mission usually uses more than two impulses. Due to the long-duration, multi-impulse characteristics, the design variables (e.g. the maneuver time) have large search space, and many sub-optimal solutions may exist, thus it is difficult to find the global optimal solution for this problem even though the state-of-art optimization algorithm is used. In addition, numerical integration of the $J_2$-perturbed trajectory is required in the optimization process, which makes the optimization time-consuming. The feasible optimization approach we used will be presented in Sec. VI.

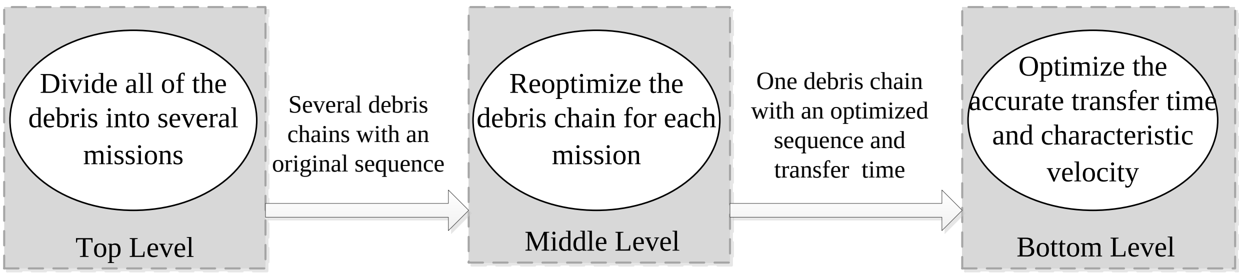


Figure 1 Interaction process among the three levels

# III. Optimization Framework

Based on the analysis in Sec. II, the whole optimization framework is mainly divided into three levels, which is illustrated in Fig. 1:

- Top Level: Divide all the debris into several missions, with each mission having a group of sequentially numbered debris.
- Middle Level: For a single mission, reoptimize the rendezvous sequence of the debris, this rendezvous sequence can be different from the one obtained in the up-lever.
- Bottom Level: Optimize the accurate transfer time and characteristic velocity for each rendezvous from one debris to another.

Three separated optimization models and algorithms are developed for each level, which are all encoded in C++ and some codes are paralleled using

MPI. For the top-level problem, we use the Debris_Chain_Bunching Ant Colony Optimization (DCB_ACO) algorithm, it is improved based on the classic ACO used for the successive debris-removal mission. A hybrid-encoding Genetic Algorithm (HEGA) is used in the middle level to simultaneously determine the sequence and the referenced transfer time a single rendezvous mission. For the bottom-level problem, a differential evolution (DE) algorithm together with a $J_2$-perturbed orbital targeting technique is used to optimize the orbital transfer trajectory.

# IV. Multiple Missions Optimization

The main task of this level is to divide the debris into several debris chains. An ACO variant for bunching debris chains is improved to solve this optimization sub-problem.

## A. Classic ACO

The ACO algorithm was originally inspired by the ability of biological ants to find the shortest path between their nest and a food source [7]. The fundamental working procedure of the Classical ACO, known as Ant System (AS), is shown in Algorithm 1.

**Algorithm 1**

Ant System

Pheromone trail initialization;
**while** Termination criteria not met do
    Solution construction;
    Pheromone update;
**end while**

## B. DCB_ACO

The fundamental procedure of DCB_ACO is similar to the classic ACO. The most important feature of an ACO is the design of the heuristic, which is eventually combined with the pheromone information to build solutions. We mainly present the heuristic and solution construction method of DCB_ACO in this part.

Every ant starts with a same set of debris (the debris that have not been removed are stored in an array $V$ ). For each ant, building a feasible solution should take the following steps.

**Step 1:** Set $T = T_0$ (MJD) as the start time.

**Step 2:** Initialize a new empty debris chain. Randomly select a debris from $V$ and set it as the head of the chain. Delete the corresponding debris in $V$. If $V$ becomes empty, go to step 8; otherwise, go to step 3.

**Step 3:** Starting from $T$, Estimate the orbital transfer time $\Delta T_{li}$ and the characteristic velocity $\Delta V_{li}$ between the last debris $V_l$ in the current chain and all remaining debris in $V$. Go to step 4.

**Step 4:** Copy all of the candidates that qualify for being bunched to the tail of the current chain from $V$ and deposit them into an array $U$. If $U$ is empty, go to step 7; otherwise, go to step 5.

**Step 5:** Randomly select a debris $V_d$ from $U$, delete the corresponding debris in $V$ after being bunched to the tail of the current chain. Go to step 6.

**Step 6:** Clean up $U$, set $T = T + \Delta T_{ld}$ and return to step 3.

**Step 7:** Close the current chain. If $V$ becomes empty, go to step 8; otherwise, set $T = T + \Delta T_M$ ( $\Delta T_M \in rand[35\ day, 65\ day]$ ) and return to step 2.

**Step 8:** Finish bunching, collect all of the accomplished debris chains.

In step 3, the optimal transfer time and characteristic velocity between each two debris are estimated based on the method presented in Sec. IV.C.

In step 4, the candidate refers to all of the debris in $V$ that satisfy the total fuel constraints for one mission after being bunched to the tail of the chain.

In step 5, the probability that an ant *k* will choose a debris *j* as the next debris for the current chain *b* in the partial solution *s* is given by

$$p_{bj}^{k}(s) = \begin{cases} \dfrac{\tau_{bj} \cdot \eta_j^{\beta}}{\sum\limits_{g \in U^k(s,b)} \tau_{bg} \cdot \eta_g^{\beta}}, & j \in U^k(s,b) \\ 0 & otherwise \end{cases} \tag{4}$$

where $U^k(s,b)$, coming from step 4, is the set of debris that qualify for bunching behind the current chain *b* and $\eta_j = \Delta V_{lj}$ is the heuristic value. The parameter $\alpha$ in Eq. (4) is fixed to 1 here because using the parameter $\beta$ is sufficient to reflect the weight between the pheromone information and heuristic information. $\tau_{bj}$ is the pheromone from debris *l* to debris *j*, where debris *l* is the last debris in the current chain *b*.

In step 6, $\Delta T_{ld}$ is the estimated optimal transfer time between the last debris $V_l$ in the current chain and the selected debris $V_d$.

In DCB_ACO, the evaporation parameter $\rho$ is set as 0.05and the increase of the pheromone $\Delta\tau_{ij}^{k}$ is limited to the maximum value of $0.1 * \tau_{ij}$ to avoid premature convergence.

## C. Analytical Estimation of Transfer Time and ΔV Cost

To efficiently evaluate the objective function of each pack and the overall cumulative cost, an analytical estimation model is presented based on the Gauss's form of variational equations [8].

$$\begin{cases} \Delta a = \dfrac{2}{n\sqrt{1-e^2}}\left[e\sin f\cdot\Delta v_r + (1+e\cos f)\Delta v_t\right] \\ \Delta e = \dfrac{\sqrt{1-e^2}}{na}\left[\sin f\cdot\Delta v_r + (\cos f + \cos E)\Delta v_t\right] \\ \Delta i = \dfrac{r\cos u}{na^2\sqrt{1-e^2}}\Delta v_h \\ \Delta\Omega = \dfrac{r\sin u}{na^2\sqrt{1-e^2}\sin i}\Delta v_h \\ \Delta\omega = \dfrac{\sqrt{1-e^2}}{nae}\left[-\cos f\cdot\Delta v_r + \left(1+\dfrac{r}{p}\right)\sin f\cdot\Delta v_t\right] - \cos i\cdot\Delta\Omega \\ \Delta M = n - \dfrac{1-e^2}{nae}\left[\left(2e\dfrac{r}{p} - \cos f\right)\Delta v_r + \left(1+\dfrac{r}{p}\right)\sin f\cdot\Delta v_t\right] \end{cases} \tag{5}$$

where the mean motion $n=\sqrt{\frac{\mu}{a^3}}$, the semilatus rectum $p=a\left(1-e^2\right)$.

1) Adjustment of the RAAN difference

The difference of the RAAN drift velocity between the spacecraft and the debris should be fully used. If the RAAN difference cannot be corrected naturally during the maximum rendezvous duration, an impulse perpendicular to the orbital plane can be implemented at the north or south vertex of the orbit.

$$\Delta v_h = \frac{na^2\sqrt{1-e^2}\sin i}{r}\left|\Delta\Omega\right| \tag{6}$$

2) Adjustment of the inclination difference

As the $J_2$-perturbation does not change the orbital inclination, the inclination difference must be corrected by maneuvers. An impulse perpendicular to the orbital plane can be implemented at the ascending node or descending node.

$$\Delta v = 2\frac{h}{r}\sin\frac{\left|\Delta i\right|}{2} \tag{7}$$

where $h=r^2\dot{\theta}$, $\theta$ is the argument of latitude.

3) Adjustment of the semimajor axis and eccentricity

After the spacecraft transfers to the same orbital plane with the debris, the semimajor axis and eccentricity are adjusted by two tangential impulses, respectively at the perigee and apogee. For a near circular orbit, omitting the high order terms of $e^2$, the velocity increment of the two impulses is formulated as follows.

$$\Delta v = n\frac{\Delta a - ae\Delta e}{2} \tag{8}$$

4) Estimation of rendezvous duration

The rendezvous duration should mainly come from the adjustment of the RAAN difference so as to make full use of the natural RAAN drift due to $J_2$-perturbation. The following adjustments do not need too much time. To be conservative, the rendezvous duration is roughly estimated as the duration for RAAN adjustment plus one day.

What's more, it may be noticed that the adjustment of phase difference is not included. Considering that the rendezvous duration usually lasts for several days, the velocity increment costed by phase difference adjustment prefers to be much less than the velocity increments of the other adjustments. To be conservation, an upper bound for phase difference adjustment can be directly added on the estimation result.

# V. Single Mission Optimization

## A. Optimization Model

There are two types of design variables. A solution $\boldsymbol{Y}$ is made up of a group of serial integers $\boldsymbol{Y}_1$ and a set of real numbers $\boldsymbol{Y}_2$ that consists of rendezvous orbital transfer times and service times.

$$\boldsymbol{Y} = (\boldsymbol{Y}_1, \boldsymbol{Y}_2) \tag{9}$$

where $\boldsymbol{Y}_1 = (p_1, p_2, ...p_N)$ and $\boldsymbol{Y}_2 = (dur_1, dur_2, ...dur_N;$ $ser_1, ser_2, ...ser_N)$ .

Through the sequence of its elements the serial integer vector $\boldsymbol{Y}_1$ represents a service order. The search space of $\boldsymbol{Y}_1$ is therefore discrete and its elements must be manipulated in combination.

The objective is to minimize the propellant consumed by orbital maneuvers:

$$\min\ f_2 = (m_0 - m_{dry} - Qm_{de}) \tag{10}$$

where $m_{dry}$ is the spacecraft's mass after the last removing mission and also denotes the spacecraft's dry mass.

## B. Solving Strategy

Denote the state of a spacecraft as

$$\boldsymbol{E} = (a, \theta, q_1, q_2, i, \Omega)^T \tag{11}$$

where $a$ is the semi-major axis, $i$ is the orbital inclination, $\Omega$ is the RAAN, $\theta$ is the mean argument of latitude, $e$ is the eccentricity, $\omega$ is the argument of perigee, and $q_1 = e\cos\omega$ and $q_2 = e\sin\omega$ are the modified orbital elements suitable for describing near-circular orbits.

The state variable used to express orbital differences between the spacecraft and one debris is

$$\mathbf{X} = (\Delta a / a_r, \Delta\theta, \Delta q_1, \Delta q_2, \Delta i, \Delta\Omega)^T \tag{12}$$

where the subscript "*r*" denotes the reference orbit, $\Delta a$ is the difference in semi-major axis, $\Delta\theta$ is the difference in argument of latitude, $\Delta i$ is the difference in orbital inclination, $\Delta\Omega$ is the difference in RAAN, and $\Delta q_1$ and $\Delta q_2$ give the differences in eccentricity vector.

Using first order approximations in the $q$th rendezvous operation, the state transitions of orbital element differences under the $J_2$ perturbation are given by [9]

$$\mathbf{X}(t_{qf}) = \mathbf{\Phi}(\Delta t_{q0})\mathbf{X}_0 + \sum_{j=1}^{2}\mathbf{\Phi}_v(\Delta t_{qj}, u_{qj})\Delta\mathbf{v}_{qj} \quad (13)$$

$$\mathbf{\Phi}(\Delta t_{q0}) = \begin{bmatrix} 1 & 0 & 0 & 0 & 0 & 0 \\ -\frac{3}{2}n_r\Delta t_{q0} - \frac{7}{2}C(3-4\sin^2 i_r)\Delta t_{q0} & 1 & 0 & 0 & -4C\sin(2i_r)\Delta t_{q0} & 0 \\ 0 & 0 & \cos(\dot{\omega}_{J_2}\Delta t_{q0}) & -\sin(\dot{\omega}_{J_2}\Delta t_{q0}) & 0 & 0 \\ 0 & 0 & \sin(\dot{\omega}_{J_2}\Delta t_{q0}) & \cos(\dot{\omega}_{J_2}\Delta t_{q0}) & 0 & 0 \\ 0 & 0 & 0 & 0 & 1 & 0 \\ \frac{7}{2}C\cos i_r\Delta t_{q0} & 0 & 0 & 0 & C\sin i_r\Delta t_{q0} & 1 \end{bmatrix} \quad (14)$$

$$\mathbf{\Phi}_v(\Delta t_{qj}, u_{qj}) = \begin{bmatrix} 0 & 2 & 0 \\ 0 & \left[-3n_r - 7C(3-4\sin^2 i_r)\right]\Delta t_{qj} & -4C\sin(2i_r)\cos u_{qj}\Delta t_{qj} \\ \sin(u_{qj} + \dot{\omega}_{J_2}\Delta t_{qj}) & 2\cos(u_{qj} + \dot{\omega}_{J_2}\Delta t_{qj}) & 0 \\ -\cos(u_{qj} + \dot{\omega}_{J_2}\Delta t_{qj}) & 2\sin(u_{qj} + \dot{\omega}_{J_2}\Delta t_{qj}) & 0 \\ 0 & 0 & \cos u_{qj} \\ 0 & 7C\cos i_r\Delta t_{qj} & \frac{\sin u_{qj}}{\sin i_r} + C\sin i_r\cos u_{qj}\Delta t_{qj} \end{bmatrix} \quad (15)$$

where $C = \frac{3J_2R_E^{\ 2}}{2}\sqrt{\mu}a_r^{-\frac{7}{2}}$ , $n_r = \sqrt{\frac{\mu}{a_r^3}}$ is the mean angular motion rate, and $\dot{\omega}_{J_2} = C\left(2 - \frac{5}{2}\sin^2 i_r\right)$ is the drift rate of perigee. $\Delta t_{q0} = t_{qf} - t_{q0} = dur_q$ is orbital transfer time, $\Delta t_{qj} = t_{qf} - t_{qj}$ , $u_{qj}$ is the argument of latitude of the *j*th maneuver, and $\Delta\boldsymbol{v}_{qj} = \left(\Delta v_{qjx}, \Delta v_{qjy}, \Delta v_{qjz}\right)^T$ is the impulse vector. The orbital coordinate system used to describe the impulse is given as follows: $x$ is along the orbital radial direction, $y$ is along the in-track direction, and $z$ is along the orbital normal direction and completes the rand-handed system. The last maneuver is executed at $t_{qf}$ , i.e. $t_{qf} = t_{q2}$ .

Eq. (13) is a linear relative dynamic equation under the $J_2$ perturbation. In this study, only two maneuvers are considered for each orbital transfer that six unknown impulse components correspond to six equations, and then the solution to Eq. (13) can be easily obtained using Gaussian elimination. The details of this linear dynamics model can be found in the references [10] and [9].

Long-duration rendezvous problems under the $J_2$ perturbation have multiple local minima both in the duration of one orbital period and in the duration of multiple orbital periods [9]. In order to overcome the property of multiple local minima in one orbital period, the burn time of the first maneuver $t_{q1}$ is enumerated from $t_{q0}$ to $t_{q0} + T_r$ with a step of $T_r / N_{enum}$ , where $T_r$ is the reference orbital period and $N_{enum}$ is the number of enumerations. For each value of $t_{q1}$ , a group of values for $\Delta\boldsymbol{v}_{q1}$ and $\Delta\boldsymbol{v}_{q2}$ can be obtained, and is referred to as $\Delta\boldsymbol{v}_{q1}(t_{q1})$ and $\Delta\boldsymbol{v}_{q2}(t_{q1})$ . The $N_{enum} + 1$ groups of $\Delta\boldsymbol{v}_{q1}(t_{q1})$ and $\Delta\boldsymbol{v}_{q2}(t_{q1})$ in total are calculated and then are compared with each other to find the group with the local minimum value of $\left\|\Delta\boldsymbol{v}_{q1}(t_{q1})\right\| + \left\|\Delta\boldsymbol{v}_{q2}(t_{q1})\right\|$ , and the values of the $\Delta\boldsymbol{v}_{q1}$ and $\Delta\boldsymbol{v}_{q2}$ in this group are used as the impulses for the orbital transfer of the *q*th rendezvous.

Based on the model provided above, the maneuver impulses of each rendezvous orbital transfer are only functions of the initial state, the required ending state and the orbital transfer time, and then the propellant cost can be evaluated with small computation cost.

## C. Optimization Algorithm

A hybrid-encoding genetic algorithm (HEGA) is adopted to solve the formulated approximated sub-problem. This algorithm is a combination of an integer-coded GA for classical TSPs [11] and the real-coded genetic algorithm [12].

The design variable vector $\boldsymbol{Y} = (\boldsymbol{Y}_1, \boldsymbol{Y}_2)$ is used directly as the chromosome of an individual. The fitness assignment process for a single-objective problem is straightforward. The arithmetical crossover and non-uniform mutation operators are applied to $\boldsymbol{Y}_2$ [12], while the ordered crossover (OX) and three-point displacement mutation operators are both applied to $\boldsymbol{Y}_1$ [11]. An elitist strategy is employed alongside tournament selection during the algorithm's selection phase. This can help prevent the loss of good solutions once they have been found [12].

# VI. Single Rendezvous Trajectory Optimization

Once the rendezvous sequence for each mission is determined using the methods given in Secs. IV and V, an optimization model is required for minimizing the $\Delta V$ cost for every single rendezvous between two debris. The orbital transfer from debris to debris is a multi-impulse, perturbed rendezvous problem under the dynamics of Eq. (2). Orbital targeting algorithms based on two-body dynamics, such as the relative-orbit-element based relative motion equations and the Lambert algorithm, cannot directly obtain a feasible solution unless some differential corrections or simple iterations are employed. In order to efficiently find a near-optimal solution for the given long-duration (up to 30 days) rendezvous problem, a feasible iteration optimization model is used, in which the homotopic perturbed Lambert algorithm [5, 14] is employed as orbital targeting algorithm. The optimization model is given in this section.

## A. Design variables

There are 4*n* design variables for an *n*-impulse maneuver plan:

$$\boldsymbol{D} = [t_i, \Delta v_{ix}, \Delta v_{iy}, \Delta v_{iz}],\ i = 1,2,...,K \quad (16)$$

where $K$ is the maneuver number of times, $t_i$ is the $i^{\text{th}}$ maneuver time, and $\Delta \boldsymbol{v}_i = [\Delta v_{ix}, \Delta v_{iy}, \Delta v_{iz}]^T$ is the $i^{\text{th}}$ maneuver impulse vector. In our results, 4-impulse maneuver plan is adopted, i.e. $K = 4$.

## B. Objective function

The objective is to minimize the total velocity increment:

$$\min J = \Delta v = \sum_{i=1}^{K} \left\| \Delta \boldsymbol{v}_i \right\| \quad (17)$$

## C. Constraints

The duration between two adjacent maneuvers should be larger than a given value, i.e.,

$$\begin{cases} t_i - t_{i-1} \geq \Delta T_i, \\ t_i \in [t_0, t_f],\ i = 1,2,...,K \end{cases} \quad (18)$$

where $t_0 = 0$, $t_f = 30$ days, $\Delta T_1 = 5$ days, $\Delta T_i$ can be set as zeros for $i = 2,...,K$. In addition, at the final time, the deviation between the spacecraft's state vector $\boldsymbol{x}_f = [\boldsymbol{r}_f, \boldsymbol{v}_f]^T$ and the state vector $\boldsymbol{x}_{\text{next}}$ of the next debris should be smaller than the given tolerant error, i.e.,

$$\left\| \boldsymbol{r}_f - \boldsymbol{r}_{\text{next}} \right\| \leq 100\text{ m},\ \left\| \boldsymbol{v}_f - \boldsymbol{v}_{\text{next}} \right\| \leq 1\text{ m/s} \quad (19)$$

## D. Feasible Iteration Optimization Approach

To deal with the linear inequality constraints presented in Eq. (18), a group of proportionality coefficients $\eta_1, \cdots, \eta_n \in [0,1]$ is used to substitute the maneuver times $t_1, \cdots, t_n$ as optimization variables. Then, the maneuver times can be calculated as

$$t_i = t_{i-1} + \eta_i (t_f - t_{i-1}) + \Delta T_i, \quad \text{where} \quad \begin{cases} \Delta T_1 = 5\text{ days}, \\ \Delta T_i = 0,\quad i = 2,...,K \end{cases} \quad (20)$$

To deal with the nonlinear inequality constraints presented in Eq. (24), the last two impulses $\Delta \boldsymbol{v}_{n-1}$ and $\Delta \boldsymbol{v}_n$ are chosen to satisfy the nonlinear inequality constraints, and that they are obtained by solving a perturbed two-point boundary value problem. Here the homotopic perturbed Lambert algorithm proposed by Yang et al. [5,14] is employed to compute these two impulses as described by:

$$(\Delta \boldsymbol{v}_{K-1}, \Delta \boldsymbol{v}_K) = Lambert\_p\left( \boldsymbol{x}(t_{K-1}), \boldsymbol{x}(t_K), t_K - t_{K-1} \right) \quad (21)$$

where $\boldsymbol{x}(t_K) = \boldsymbol{x}_{\text{next}}$, and the position and velocity error tolerances for the perturbed Lambert algorithm are respectively set as 100 m and 1 m/s. This perturbed Lambert algorithm allowed the perturbed solutions that included the successful computation of the $J_2$-perturbation through a homotopic targeting technique in which the two-body Lambert solution was used as an initial value and the Runge-Kutta integration of Eq. (2) was used as a perturbed trajectory propagator.

Overall, the optimization model for a multiple-impulse rendezvous problem can be rewritten as follows based on the feasible iteration approach:

$$\min_{\boldsymbol{X}} J = \sum_{i=1}^{n} \left\| \Delta \boldsymbol{v}_i \right\|, \text{ subject to}$$
$$\left\| \boldsymbol{r}_f - \boldsymbol{r}_{\text{next}} \right\| \leq 100\text{ m},\ \left\| \boldsymbol{v}_f - \boldsymbol{v}_{\text{next}} \right\| \leq 1\text{ m/s, where}$$
$$\begin{cases} \boldsymbol{X} = \left[ \eta_1, \cdots, \eta_K, \Delta \boldsymbol{v}_1, \cdots, \Delta \boldsymbol{v}_{K-2} \right], \\ \eta_i \in [0,1], t_i = t_{i-1} + \eta_i (t_f - t_{i-1}) + \Delta T_i,\quad i = 1,...,K \\ (\Delta \boldsymbol{v}_{K-1}, \Delta \boldsymbol{v}_K) = Lambert\_p\left( \boldsymbol{x}(t_{K-1}), \boldsymbol{x}(t_K), t_K - t_{K-1} \right) \end{cases} \quad (22)$$

Although the optimization problem presented in Eq. (28) is formulated as an unconstrained problem, it is very difficult to solve directly with a gradient-based method such as SQP algorithm because these algorithms are very sensitive to the initial guess. Moreover, the long duration and probably large non-coplanar difference of RAAN make it very difficult to obtain the optimal solution for the rendezvous problem. Therefore, it is highly desirable and necessary to employ a global optimization algorithms that do not require any gradient information or initial guess to solve the problem. We use a differential evolution (DE) algorithm [16] to solve the optimization model of Eq. (22).

# VII. Simulation Results

The start and end epoch as well as the debris removal sequence for each mission are listed in Table 1. It can be found that all the 123 debris are removed in 12 missions. The numbers of debris removed in each mission are mainly between seven and twelve except for 17 of the first mission.

Table 1 Events epochs and debris removal sequences

| Mission Order | Start Epoch (MJD) | End Epoch (MJD) | Debris Number | Debris Removal Sequence | Start Mass (kg) |
|---|---|---|---|---|---|
| 1 | 23517.00 | 23811.52 | 17 | 0, 115, 12, 67, 19, 48, 122, 7, 63, 61, 82, 107, 41, 11, 45, 85, 47 | 5478.12 |
| 2 | 23893.80 | 24092.29 | 11 | 58, 28, 90, 51, 72, 69, 10, 66, 73, 64, 52 | 4106.88 |
| 3 | 24122.30 | 24427.74 | 12 | 84, 86, 103, 16, 121, 92, 49, 23, 20, 54, 27, 36 | 3809.97 |
| 4 | 24461.50 | 24660.15 | 10 | 8, 43, 9, 55, 95, 14, 102, 39, 113, 110 | 4081.09 |
| 5 | 24785.00 | 24975.41 | 12 | 83, 75, 22, 35, 119, 24, 108, 37, 112, 104, 32, 114 | 5782.68 |
| 6 | 25006.00 | 25198.32 | 9 | 118, 65, 74, 50, 94, 21, 97, 79, 120 | 4024.43 |
| 7 | 25281.60 | 25454.87 | 10 | 62, 1, 40, 76, 89, 99, 15, 59, 98, 116 | 4877.61 |
| 8 | 25555.40 | 25669.64 | 8 | 117, 91, 93, 70, 18, 105, 88, 46 | 4909.98 |
| 9 | 25702.40 | 25860.22 | 9 | 5, 53, 33, 68, 71, 80, 57, 60, 106 | 4419.99 |
| 10 | 25912.74 | 26055.85 | 8 | 2, 81, 96, 6, 100, 30, 34, 26 | 3902.24 |
| 11 | 26087.53 | 26262.18 | 10 | 87, 29, 101, 31, 38, 25, 4, 77, 13, 3 | 4267.35 |
| 12 | 26292.26 | 26381.58 | 7 | 44, 111, 56, 78, 17, 109, 42 | 3584.37 |

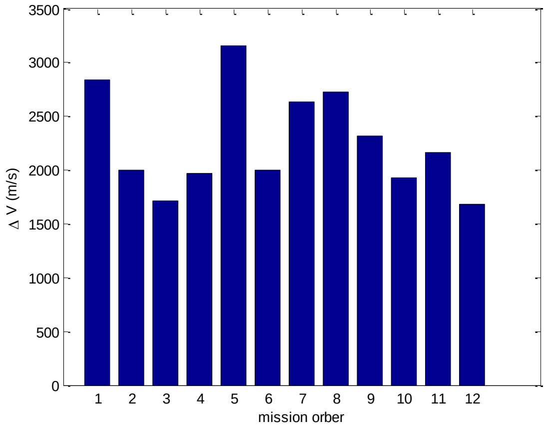


Figure 1 Total $\Delta V$ of each mission

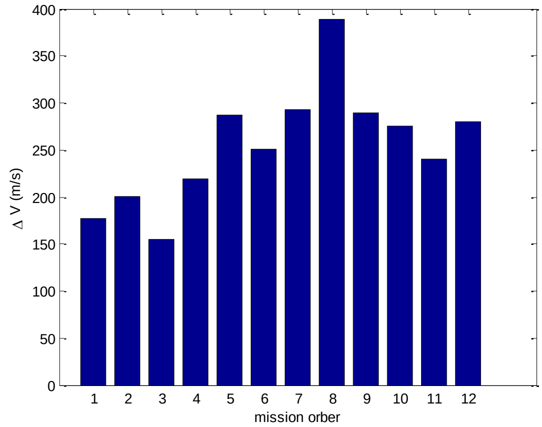


Figure 2 Average $\Delta V$ of each mission

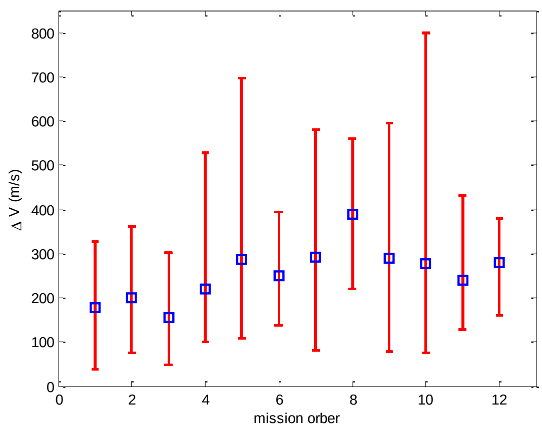


Figure 3 Minimum and maximum $\Delta V$ of each mission

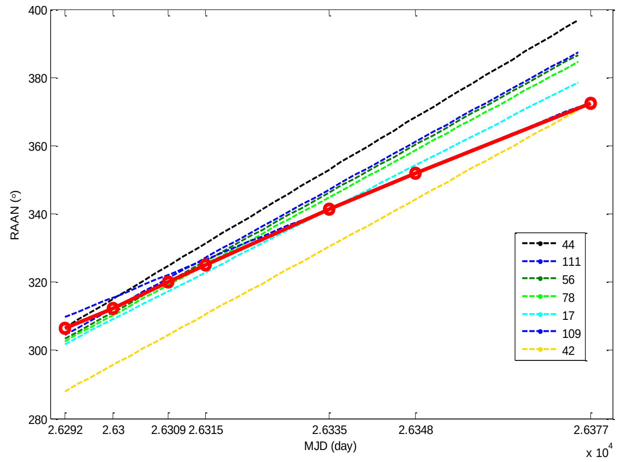


Figure 4 History of the RAAN of the active spacecraft and corresponding debris for mission #12

The total velocity increments for rendezvous of each mission are presented in Fig. 1. As is shown, the total velocity increments of most missions are between 1500 m/s and 2500 m/s while only that of the fifth mission is beyond 3000 m/s. However, it should be noticed that the first mission has also removed the most debris. The average velocity increments of each mission are better indices to evaluate the performance of each mission. As is shown in Fig. 2, the average velocity increments of the first four missions are below 250 m/s, while for most of other missions the average velocity increments are near 300 m/s, which indicates that the performances of the first four missions are better than others. It is clear that the average velocity increment of the eighth mission is the largest with a number of near 400 m/s, which indicates that the mission is not optimal. The minimum and maximum velocity increments of each mission are illustrated in Fig. 3. According to Fig. 3, the smallest velocity increment of all 12 missions is 38.6 m/s while the largest one is 798.3 m/s. It can be indicated that the range of velocity increments for a single rendezvous process of each mission is very wide.

The histories of the RAAN of the active spacecraft and corresponding debris removed in the last mission are shown in Fig. 4, where the red line with circles indicated the history of RAAN of the spacecraft. It can be found that the RAAN of the spacecraft increases gradually as it rendezvouses the debris one by one. The RAAN of debris 42, as shown in the Fig. 4, is not close to other debris in this sequence, but there is an intersection between it and that of debris 109 at the MJD around 26377. Consequently, it is clear that the spacecraft waits to that epoch to rendezvous with debris 42 from debris 109 so as to reduce the velocity increments for maneuvers caused by a large initial RAAN error.

# V. Conclusions

A three-level optimization framework is presented to solve the problem of GTOC9, wherein the competitors are called to design a series of missions able to remove a set of 123 orbiting debris pieces while minimizing the overall cumulative cost. The top level is similar to a dynamic TSP, wherein the debris pieces are divided into several groups and each group of debris is removed by one mission. The middle level is a mixed-integer optimization problem, wherein the impulses and durations of each rendezvous in one mission are designed. And the bottom level is the precise and detailed optimization of the flight trajectory in one rendezvous. The result of GTOC9 obtained by this framework is then illustrated. The result indicates that the three-level optimization framework is efficient and can obtain good solutions in considerable time.

# References


[1] GTOC Portal, https://sophia.estec.esa.int/gtoc_portal/

[2] GTOC9 Homepage, https://kelvins.esa.int/gtoc9-kessler-run/

[3] Izzo D, Getzner I, Hennes D, et al. “Evolving solutions to TSP variants for active space debris removal,” Proceedings of the 2015 Annual Conference on Genetic and Evolutionary Computation, ACM, 2015: 1207-1214.

[4] Zhang, J., Parks, G. T., Luo, Y., Tang, G. “Multispacecraft Refueling Optimization Considering the J2 Perturbation and Window Constraints,” Journal of Guidance, Control, and Dynamics, Vol. 37, 2014, pp. 111–122.

[5] Yang, Z., Luo, Y.-Z., Zhang, J., Tang, G.J. “Homotopic Perturbed Lambert Algorithm for Long-Duration Rendezvous Optimization,” Journal of Guidance, Control, and Dynamics, Vol. 38, No. 11, 2015, pp. 2215–2223.

[6] Yang, Z., Luo, Y. Z., Zhang, J., “Two-level Optimization Approach for Mars Orbital Long-Duration, Large Non-Coplanar Rendezvous Phasing Maneuvers,” Advances in Space Research, Vol. 52, 2013, pp. 883–894.

[7] Dorigo M., Gambardella L.M., “Ant Colony System: A cooperative learning approach to the traveling salesman problem,” IEEE Transactions on Evolutionary Computation, Vol. 1, No. 1, 1997, pp. 53-66.

[8] Luo Y.Z., Li H.Y., Tang G.J. "Hybrid Approach to Optimize a Rendezvous Phasing Strategy", Journal of Guidance, Control, and Dynamics, Vol. 30, No. 1, 2007, pp. 185-191.

[9] Zhang, J., Luo, Y. Z., and Tang, G. J., “Hybrid Planning for LEO Long-Duration Multi-Spacecraft Rendezvous Mission,” Science China Technological Sciences, Vol. 55, No. 1, 2012, pp. 233–243.

[10] Labourdette, P., and Baranov, A. A., “Strategies for on-orbit rendezvous circling Mars,” Advances in the Astronautical Sciences, Vol. 109, 2002, pp.1351–1368.

[11] Chatterjee S., Carreraa, C., and Lynch L. A., “Genetic Algorithms and Traveling Salesman Problems,” European Journal of Operational Research, Vol. 93, No. 3, 1996, pp. 490–510.

[12] Deb, K., Pratap, A., Agarwal, S., and Meyarivan, T., “A Fast and Elitist Multi-Objective Genetic Algorithm: NSGA-II,” IEEE Transactions on Evolutionary Computation, Vol. 6, No. 2, 2000, pp. 182–197.

[13] Yang, Z., Luo, Y. Z., and Zhang, J., “Robust Planning of Nonlinear Rendezvous with Uncertainty,” Journal of Guidance, Control, and Dynamics, in press.

[14] Luo, Y. Z., Zhang, J., and Tang, G. J., “Survey of Orbital Dynamics and Control of Space Rendezvous,” Chinese Journal of Aeronautics, Vol. 27, No. 1, 2014, pp. 1–11.

[15] Luo, Y. Z., Tang, G. J., Lei, Y. J., et al., “Optimization of Multiple-Impulse, Multiple -Revolution, Rendezvous-Phasing Maneuvers,” Journal of Guidance, Control and Dynamics, Vol. 30, No. 4, 2007, pp. 946–952.

[16] Zhu Y. H., Wang H., and Zhang J., “Spacecraft Multiple-Impulse Trajectory Optimization Using Differential Evolution Algorithm with Combined Mutation Strategies and Boundary-Handling Schemes,” Mathe. Probl. Engi., 2015.